

Characterization of third-harmonic generation in Fibonacci optical superlattices

Xianjie Liu, Zhenlin Wang, and Jun Wu

National Laboratory of Solid State Microstructures, Nanjing University and Center for Advanced Studies in Science and Technology of Microstructures, Nanjing 210093, China

Naiben Ming

National Laboratory of Solid State Microstructures, Nanjing University and Center for Advanced Studies in Science and Technology of Microstructures, Nanjing 210093, China

and China Center for Advanced Science and Technology (World Laboratory), P.O. Box 8730, Beijing 100080, China

(Received 5 November 1997)

A Fibonacci optical superlattice (FOS) made from a single crystal with a quasiperiodic laminar ferroelectric domain structure was proposed to realize a third-harmonic generation (THG) process. Due to its quasiperiodic structure, a FOS can provide more plentiful reciprocal-lattice vectors to compensate for the mismatch phase in optical parametric processes, which causes most of third-harmonic peaks labeled by the corresponding reciprocal-lattice vector indices. Numerical calculation shows that the THG spectrum exhibits a self-similarity property in real space. Effects of the phase mismatch of second-harmonic generation and THG, the bandwidth, and the relative intensity of the second harmonic peak on THG are discussed. We also found THG peaks for which the quasi-phase-matching condition in THG process is not completely satisfied. The physical origins of the phenomenon are presented and discussed. [S1050-2947(98)07612-4]

PACS number(s): 42.65.Ky, 77.80.Dj

I. INTRODUCTION

Recently, much attention has been paid to harmonic generation, especially to second-harmonic generation (SHG) [1–5]. Traditionally, harmonic generation is produced by phase matching using the birefringence of nonlinear crystals. Such an approach limits the range of frequencies which can be used to generate harmonics and the choice of nonlinear coefficients. On the other hand, it is difficult to realize high-order harmonic generation by the traditional method. One solution is quasi-phase-matching (QPM) [6,7], which is known as an attractive way to obtain good phase matching, and has been studied intensively [5]. With the QPM technique, phase matching becomes possible at ambient temperature and does not introduce spatial walk-off; the polarization with the largest nonlinearity can be used, and materials with larger nonlinearities can be exploited, which are not phase matchable by angle or temperature tuning. The physics of QPM involves constructing a periodic structure with the phase of nonlinear polarization shifted from one lamina to the next by a π radian along the direction of propagation. Since the nonlinear-optical coefficient forms a third-rank tensor, it will change the signs from positive domains to negative ones [8]. As a result, the nonlinear coefficient in the superlattice is modulated with a periodic sign reversal, by which an additional (grating) vector is introduced. In optical parametric processes, the additional vector can compensate for the mismatch between the wave vectors of the fundamental and harmonic waves. Although this approach does not allow a perfect phase match between the fundamental and harmonic, it can lead to quasi-phase-matchable harmonic generation. In past few years, the experimental difficulties in QPM have been overcome and stable techniques have been developed, such as domain inversion, proton exchange, and

etching and cladding in ferroelectric material, to mention a few.

Usually, periodic optical superlattices provide a series of reciprocal-lattice vectors, which is an integer times a primitive vector. In a quasiperiodic Fibonacci optical superlattice (FOS), however, the reciprocal-lattice vectors are governed by two integers rather than by one integer as in the case of the periodic one. Therefore, the superlattice can provide more reciprocal-lattice vectors, which will make the optical parametric processes in the FOS more colorful than in the periodic superlattice. These parametric processes can be efficiently realized in the superlattice.

In this paper, we report our theoretical results on third-harmonic generation (THG) in a Fibonacci optical quasiperiodic superlattice. We study the dispersion relation effects on THG, and the spectrum of the THG intensity in real and reciprocal spaces. We found that most of the intense third-harmonic peaks can be labeled by indices of the reciprocal-lattice vectors, but some of them are not labelable. The physical conditions for efficient THG are presented and discussed. By properly designing the parameter of a FOS, THG at a desired output wavelength, with a strong intensity, can be realized.

II. THEORETICAL ANALYSIS

Let us construct a FOS. First, two building blocks A and B with thicknesses l_A and l_B , respectively, are defined. Each block is composed of two ferroelectric domains with opposite polarization [see Fig. 1(a)]. Let l_A^+ (l_A^-) and l_B^+ (l_B^-) represent the thickness of the positive (negative) domains in blocks A and B . We assume that

$$l_A = l_A^+ + l_A^-, \quad l_B = l_B^+ + l_B^-, \quad (1)$$

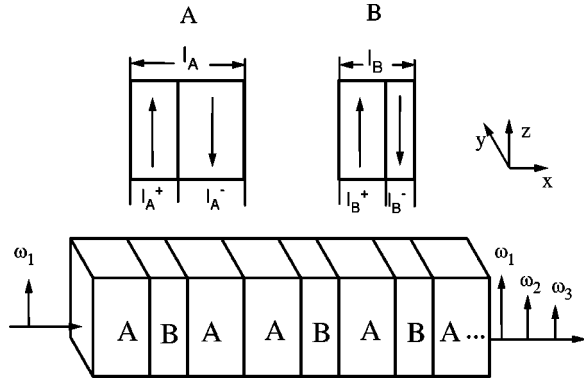


FIG. 1. Schematic diagram of the unit blocks A and B in the construction of the FOS and the sequence of the FOS. The arrows in each block represent the direction of domain polarization.

with $l_A^+ = l_B^+ = l$, and define the parameters t and δ by

$$l_A^- = l(1 + \delta), \quad l_B^- = l(1 - \delta). \quad (2)$$

It is well known that the substitution rules of a Fibonacci sequence are $A \rightarrow AB$ and $B \rightarrow A$. The corresponding production rule is $S_j = S_{j-1} + S_{j-2}$ for $j > 2$ with $S_1 = \{A\}$ and $S_2 = \{AB\}$. We arrange blocks A and B as the sequence of $ABAABABA\dots$. Thus a FOS is established, as shown in Fig. 1(b).

The optical wave propagation in the FOS can be obtained from the small-signal approximation [4,9]. A pump beam with frequency $\omega_1 = \omega$ is incident normal to the superlattice surface from the left along the x axis, with the electric field aligned along the z axis. The domain walls are parallel to the y - z plane [see Fig. 1(b)]. With this geometry, the largest nonlinear coefficient d_{33} is exploited. The second harmonic with $\omega_2 = 2\omega$ and the third harmonic with $\omega_3 = 3\omega$ are produced via the optical parametric processes. The electric fields at the three frequencies are described as $E_i(x, t) = E_i(x) \exp[i(\omega_i t - k_i x)]$ ($i = 1, 2, 3$). The nonlinear polarizations at ω_2 and ω_3 are

$$P_{2\omega}(x, t) = 2d(x)E_1^2(x) \exp[i(2\omega_1 t - 2k_1 x)], \quad (3a)$$

$$P_{3\omega}(x, t) = 4d(x)E_1(x)E_2(x) \times \exp\{i[(\omega_1 + \omega_2)t - (k_1 + k_2)x]\}, \quad (3b)$$

where $d(x)$ is the modulated nonlinear optical coefficient, $d(x) = d_{33}$ if x is in the positive domains, and $d(x) = -d_{33}$ elsewhere.

In this paper, we only consider a second-order process in which the second-harmonic generation occurs as a result of two incident beams mixing, and THG is due to sum frequency of the fundamental and the second harmonic. From Maxwell's equations, using the small-signal approximation and assuming the undepleted input beam, i.e., $k_i dE_i(x)/dx \gg d^2 E_i(x)/dx^2$, $dE_1(x)/dx = 0$, and $E_1(x) \gg E_2(x)$ and $E_3(x)$, we obtain [4,9]

$$\frac{dE_2(x)}{dx} = -i \frac{4\pi\omega_2^2}{k_2 c^2} d(x)E_1^2(x) \exp(i\delta k_2 x), \quad (4a)$$

$$\frac{dE_3(x)}{dx} = -i \frac{8\pi\omega_3^2}{k_3 c^2} d(x)E_1(x)E_2(x) \exp(i\delta k_3 x), \quad (4b)$$

with

$$\delta k_2 = k_2 - 2k_1 = 4\pi(n_2 - n_1)/\lambda, \quad (5a)$$

$$\delta k_3 = k_3 - k_2 - k_1 = (6\pi n_3 - 4\pi n_2 - 2\pi n_1)/\lambda, \quad (5b)$$

where δk_2 and δk_3 are the phase mismatches in SHG and THG, respectively. In Eq. (5), n_1 , n_2 , and n_3 are the refractive indices for the fundamental, second harmonic, and third harmonic, respectively. By numerical calculation, we can obtain the intensity of SHG and THG. In the following discussion, we use KTiOPO₄ crystal as an example, the refractive indices of which as functions of wavelength at room temperature are taken from Ref. [10]. The intensities of the second and third harmonics are all normalized to a unit for the intensity of the fundamental wave $|E_1|^2$ with $|d_{33}E_1|^2 = 10^{-14}$.

In the integration of $E_2(x)$ and $E_3(x)$, the most important factor is the modulated nonlinear coefficient $d(x)$. Being a Fibonacci distribution function, it has an important effect on the harmonic intensity. So before discussing the harmonic generation properties of the FOS, we first analyze the function $d(x)$ of the structure. It is known that the Fourier transform of $d(x)$ can be obtained by the direct [11] or the projection [12] method for an infinite array, and can be written as [2]

$$d(x) = \sum_{m,n} d_{33} \frac{\sin(1/2kl)}{1/2kl} \frac{\sin X_{m,n}}{X_{m,n}} \delta(k - G(m,n)) \exp(ikx) = \sum_{m,n} d_{m,n} \exp[iG(m,n)x], \quad (6)$$

with

$$X_{m,n} = \pi \tau^2 (ml_A - nl_B) / D,$$

$$D = \tau l_A + l_B,$$

$$G(m,n) = 2\pi(m+n\tau) / D,$$

where $G(m,n)$ is the reciprocal-lattice vectors of a FOS. If these vectors can compensate for the phase mismatches in optical parametric processes for a pump beam, a peak of harmonics will appear at that wavelength. In Eq. (6), the Fourier transformation coefficient $d_{m,n}$ is defined as the effective nonlinear coefficient of the superlattice, which contains two factors $\sin[1/2G(m,n)l]/1/2G(m,n)l$ and $\sin X_{m,n}/X_{m,n}$. For the factor $\sin[1/2G(m,n)l]/1/2G(m,n)l$, the smaller the indices of m and n , the larger the value of the former term. The factor $\sin X_{m,n}/X_{m,n}$ depends on m and n in the manner that, as $ml_A - nl_B$ approaches zero, i.e., $n/m \rightarrow l_A/l_B$, the value of $\sin X_{m,n}/X_{m,n}$ approaches unity, which is the largest value the factor can take.

THG occurs as a result of sum frequency of the fundamental and the second harmonic. Its intensity depends on

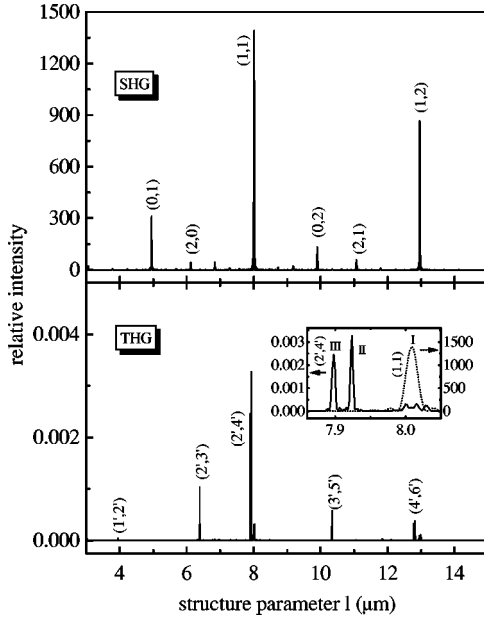


FIG. 2. The dependence of the third-harmonic spectrum on the structure parameter l , with $t=1.7$, $\delta=0.36$, and $\lambda=1.3 \mu\text{m}$, and the corresponding second-harmonic spectrum. The inset is the enlarged intensity spectrum, and the dashed line stands for the corresponding SHG spectrum.

three factors— $d(x)$, $E_2(x)$, and phase mismatch δk_3 —for a fixed intensity of the pump beam. When the QPM SHG condition is satisfied, i.e.,

$$\Delta K_2 = \delta k_2 - G(m, n) = 0, \quad (7)$$

where ΔK_2 is quasi-phase mismatch in SHG process, the second-harmonic peaks will appear in the harmonic generation spectrum of the structure, and the spectrum is then labeled by indices (m, n) of the reciprocal-lattice vector $G(m, n)$. If there is another reciprocal-lattice vector $G(m', n')$ which can satisfy the QPM THG condition, i.e.,

$$\Delta K_3 = \delta k_3 - G(m', n') = 0, \quad (8)$$

where ΔK_3 is a quasi-phase-mismatch in the THG process, a THG peak will occur simultaneously for the pump beam. This implies that in this case the third-harmonic peak can be labeled by two types of indices (m, n) and (m', n') .

III. NUMERICAL RESULTS AND DISCUSSIONS

Now we turn our attention to discuss the fascinating phenomena of third-harmonic spectra in real and reciprocal spaces. In real space, we keep the incident wavelength λ_0 fixed. Then the dispersive relation will have no effect on the third-harmonic spectrum. Figure 2 shows the dependence of the third harmonic on structure parameter l , in which the indices without prime in circular bracket is for SHG, and those with prime is for THG. From the QPM THG condition of Eq. (8), the third-harmonic peaks occur at

$$l(m', n') = \frac{(m' + n' \tau) \lambda_0}{(6n_3 - 4n_2 - 2n_1)(1 + \tau + (\tau - t) \delta / 2)}. \quad (9)$$

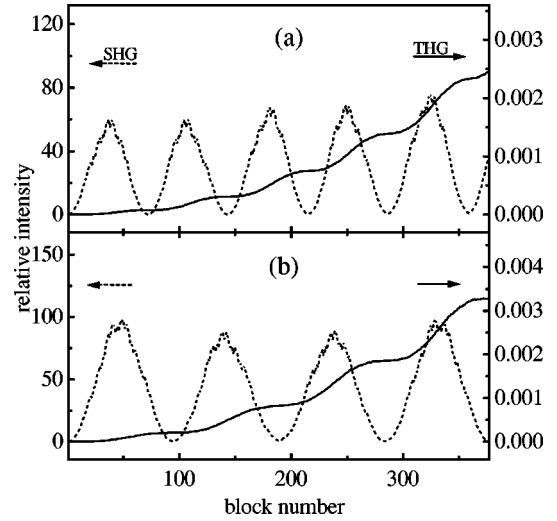


FIG. 3. The relation between the THG intensity and block number for peaks III ($2', 4'$), and II shown in (a) and (b), respectively. The dashed line in each figure is the corresponding SHG intensity distribution.

Thus the spectrum exhibits self-similarity, a characteristic of the Fibonacci sequence. From Fig. 2, it is clear that the relation $l(3', 5') = l(1', 2') + l(2', 3')$ holds. The second-harmonic spectrum also has this kind of property.

In addition, in Fig. 2, most of the THG peaks occur without a corresponding SHG peak. This is obviously because the situations of THG QPM can be frequently met, whereas a simultaneous occurrence of QPM in both SHG and THG rarely occurs by changing the structure parameter l . We can understand the phenomenon by plotting the dependence of the intensity on block number within the superlattice for these THG peaks. Figure 3(a) shows the intensity distribution of third-harmonic intense peak ($2', 4'$) at $l=7.898 \mu\text{m}$ within the FOS. For comparison, the corresponding second-harmonic intensity distribution in the structure is also plotted. As Fig. 3(a) shows, the third-harmonic intensity accumulates in a stepwise manner, whereas the second-harmonic intensity fluctuates periodically. In this case the second-harmonic process is severely quasi-phase-mismatched, but the third harmonic is quasi-phase-matched. One stage in third-harmonic intensity corresponds to every oscillation in second-harmonic intensity. When the second-harmonic intensity varies in the vicinity of a trough, a stage appears in the third-harmonic intensity. So we believe that the compensation of δk_3 is more important than that of δk_2 for an efficient THG process. If the third harmonic is quasi-phase-matched, the third harmonic still may have a stronger intensity, even though the second harmonic is quasi-phase-mismatched.

In Fig. 2, there is a special THG peak, i.e., the THG peak at $l=7.924 \mu\text{m}$, with a rather stronger intensity that cannot be labeled by THG or SHG indices. To understand the phenomenon, we have enlarged the SHG and THG spectra near the peak, and we present them in the inset of Fig. 2. It can be seen that the unlabeled THG peak II is sandwiched by two labeled peaks, i.e., the left THG peak III ($2', 4'$) at $l_{\text{III}}=7.898 \mu\text{m}$ and the right SHG peak I ($1, 1$) at $l_I=8.01 \mu\text{m}$. The intensity distribution of peak II is shown in Fig. 3(b), where the third harmonic still has a stronger intensity with

steplike increase behavior. Compared with the intensity distributions of peaks III in Fig. 3(a), peak II has a lower stage number in the THG process. It is further found that the positions of SHG peak (1,1), the unlabeled THG peak II, and THG peak (2',4') satisfy a special relation

$$(l_I - l_{II}) / (l_{II} - l_{III}) = l^{2c} / l^{3c}, \quad (10)$$

where l_i ($i=I,II,III$) are the positions of the corresponding peaks in the inset of Fig. 2, and l^{2c} and l^{3c} are the coherence lengths for the second and third harmonics at pump $\lambda_0 = 1.3 \mu\text{m}$ used in the calculation of Fig. 2, respectively. This means that the absolute value of the quasi-phase-mismatch in THG is the same as that in SHG, i.e., $\Delta K_3 + \Delta K_2 = 0$. In this case a THG peak with a larger intensity appears in the spectrum.

It is noted that the peak positions of the second and third harmonics in real space change with the parameters δ if t is not equal to the golden ration τ . This is because the parameter $D = 2(1 + \tau + (\tau - t)\delta/2)l$ changes with the variation of δ if $t \neq \tau$, and so do the reciprocal-lattice vectors $G(m,n) = 2\pi(m+n\tau)/D$. Only when $t = \tau$ do the positions of SHG and THG peaks not change with the variation of δ [3,13]. This provides us a method to optimize the structure parameter of a FOS to achieve SHG or THG at a desired wavelength.

In reciprocal-lattice space, the structure parameter l is kept constant. The harmonic generation spectra are obtained by changing the wavelength of the pump beam. Thus the dependence of refractive indices on the wavelength should be taken into account, i.e., $n_3(\lambda)$, $n_2(\lambda)$, and $n_1(\lambda)$ are functions of wavelength λ . From the QPM THG condition of Eq. (8), it is readily shown that the intense THG peaks occur at the wavelength that satisfies the relation

$$(1/\lambda)_{m',n'} = \frac{(m' + n'\tau)}{(6n_3(\lambda) - 4n_2(\lambda) - 2n_1(\lambda))D}. \quad (11)$$

The THG intensity as a function of pump wavelength is shown in Fig. 4. It is clearly seen that the relation $(1/\lambda)_{2',4'} = (1/\lambda)_{2',3'} + (1/\lambda)_{0',1'}$ is no longer held due to the dispersive effect of the optical material. The self-similarity of the Fibonacci superlattice is destroyed in reciprocal-lattice space due to optical material dispersion.

In Fig. 4, two kinds of THG peaks in real space also exist in reciprocal-lattice space; THG peaks labeled only by THG indices, and THG peaks not labeled by any indices, as shown in inset (a) of Fig. 4. The corresponding intensity distribution is presented in Figs. 5(a) and 5(b). It is noted that in Fig. 4, there is another kind of THG peak near the widest SHG peak (1,0) at $\lambda = 2.172 \mu\text{m}$. The THG peak cannot be labeled by THG indices, and its shape is enlarged and plotted in the inset (b) of Fig. 4. It is known that mismatch phases δk_2 and δk_3 in our calculated range decrease with an increase of wavelength for KTiOPO₄ crystal. When the SHG QPM condition is satisfied, an intense SHG peak with low indices will appear at the long-wavelength side with a relatively larger full width at half maximum (FWHM). These SHG peaks will influence the THG dramatically. We found that the FWHM of the second-harmonic peak (1,0) is about $0.02 \mu\text{m}$, which covers the corresponding third-harmonic peak [see inset (b)

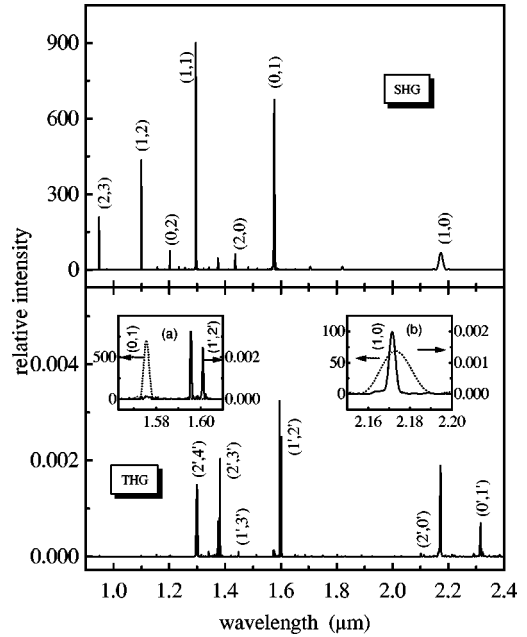


FIG. 4. The dependence of the THG spectrum on wavelength with $t = 1.75$, $\delta = 0.39$, and $l = 7.96 \mu\text{m}$, and the corresponding SHG spectrum. The two insets are the amplified THG spectra, with a dashed line for the SHG spectra.

of Fig. 4]. Although the mismatch phase of third harmonic cannot be completely compensated for by the nearest reciprocal-lattice vector $G(m',n')$ to δk_3 in the THG process, the third harmonic grows to a large intensity within the

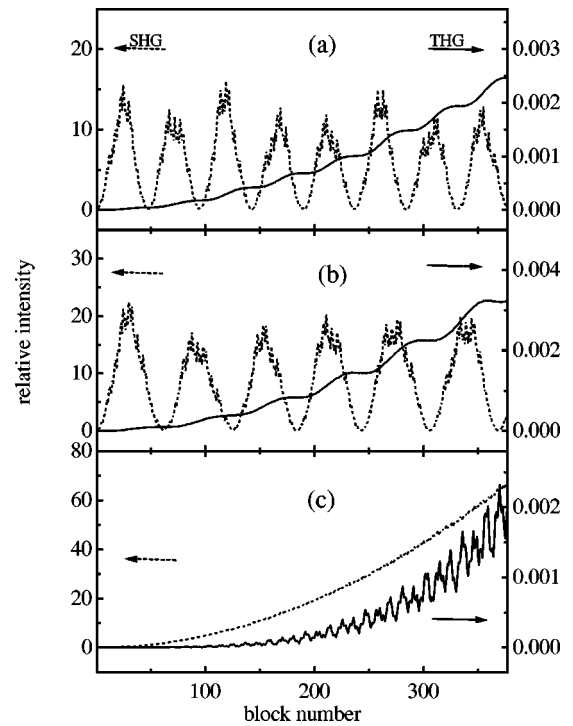


FIG. 5. The relation between THG intensity and block number for three THG peaks. (a) is for peak (1',2') at $\lambda = 1.601 \mu\text{m}$, (b) is for the unlabeled peak at $\lambda = 1.596 \mu\text{m}$ in inset (a) of Fig. 4, and (c) is for the unlabeled peak at $\lambda = 2.172 \mu\text{m}$ in inset (b) of Fig. 4. The dashed line in each figure is the corresponding SHG intensity distribution.

FOS, as the result of an intense second-harmonic peak. We plot the intensity distribution of the peak in Fig. 5(c). It can be seen that both SHG and THG intensities increase with block number, but with obvious fluctuation in THG intensity distribution, which is different from THG peaks with THG indices, but not SHG indices for which the third-harmonic intensity increases in a stepwise fashion.

From a study of the relation between the intensity spectra and the incident wavelength for different structure parameters l , we also found that the profiles of the spectra move toward the short-wavelength side with a decrease of l . For example, if we choose $l=l^{2c}(\lambda_0)$, i.e., the coherence length for SHG at wavelength λ_0 , an intense SHG peak with indices (1,1) always appears in the vicinity of wavelength λ_0 . To realize efficient harmonic generations at a short wavelength, a normal method is to decrease the domain width, especially in a periodic optical superlattice. But it is difficult to obtain very thin domains in experiment. In an optical quasiperiodic superlattice, this difficulty can be overcome. As discussed above, a multiwavelength harmonic-generation characteristic can be realized in a FOS. By properly designing the structure parameters of a FOS, we can realize harmonic generations at the desired wavelength with a stronger intensity. This provides a chance to implement compact short-wavelength coherent light sources in a FOS.

IV. CONCLUSION

In summary, we have investigated harmonic generations in the Fibonacci optical superlattice. Due to the dispersion effects of the optical material, the self-similarity of the THG harmonic spectrum in real space is destroyed in reciprocal space. In the spectrum of the third harmonic, only small positions of the peaks can be labeled by two types of indices, whereas most of intense peaks are only labeled by third-harmonic indices. We also found some peaks which cannot be labeled by any indices. For an efficient THG process, compensation of phase mismatch δk_3 is more important than that of the mismatched phase δk_2 . Other factors, such as the FWHM of the second harmonic, and its relative intensity, will also affect the THG. We also discussed the possibility of realizing the third harmonic at any wavelength by a proper choice of the structure parameter of a FOS in practical applications.

ACKNOWLEDGMENTS

This work was supported by a grant for the Key Research Project in Climbing Program from the National Science and Technology Commission of China and the National Natural Science Foundation of China. Z. L. W. was supported by the Sanzhu Company Limited in Shangdong, China.

-
- [1] M. Höue and P. D. Townsend, *J. Phys. D* **28**, 1747 (1995).
 - [2] S. N. Zhu, Y. Y. Zhu, Y. Q. Qin, H. F. Wang, C. Z. Ge, and N. B. Ming, *Phys. Rev. Lett.* **78**, 2752 (1997).
 - [3] Y. Y. Zhu and N. B. Ming, *Phys. Rev. B* **42**, 3676 (1990).
 - [4] J. Feng, Y. Y. Zhu, and N. B. Ming, *Phys. Rev. B* **41**, 5578 (1990).
 - [5] M. M. Fejer, G. A. Magel, D. H. Jundt, and R. L. Byer, *IEEE J. Quantum Electron.* **28**, 2631 (1992), and references therein.
 - [6] J. A. Armstrong, N. Bloembergen, J. Ducuing, and P. S. Pershan, *Phys. Rev.* **127**, 1918 (1962).
 - [7] N. Bloembergen and A. J. Sievers, *Appl. Phys. Lett.* **17**, 483 (1970).
 - [8] A. Yariv and P. Yeh, *Optical Waves in Crystals* (Wiley, New York, 1984).
 - [9] F. Zernike and J. M. Midwinter, *Applied Nonlinear Optics* (Wiley, New York, 1973).
 - [10] K. C. Zhang and X. M. Wang, *Nonlinear Optical Crystals Material Science* (in Chinese) (Science Press, Beijing, 1996).
 - [11] R. K. Zia and W. J. Dallas, *J. Phys. A* **18**, L341 (1985).
 - [12] D. Levine and D. J. Steinhardt, *Phys. Rev. B* **34**, 596 (1986).
 - [13] R. Merlin, K. Bajema, R. Clarks, F. Y. Juang, and P. K. Bhat-tacharga, *Phys. Rev. Lett.* **55**, 1768 (1985).